J Ind Microbiol Biotechnol (2007) 34:475–481
DOI 10.1007/s10295-007-0217-5

ORIGINAL PAPER

Optimal biocatalyst loading in a fixed bed

V. Tortoriello · G. B. DeLancey

Received: 6 September 2006 / Accepted: 8 March 2007 / Published online: 4 April 2007

Abstract The optimal distribution of biocatalyst in a fixed bed operating at steady state was determined to minimize the length of the bed for a fixed conversion of 95%. The distribution in terms of the biocatalyst loading on an inert support depends upon the axial distance from the bed entrance (continuous solution) as well as a set of dimensionless parameters that reflect the bed geometry, the bulk flow, reaction kinetics and diffusional characteristics. A mathematical model of the system with the following features was used to obtain the results: (1) convective mass transfer and dispersion in the bulk phase; (2) mass transfer from the bulk phase to the surface of the catalyst particle; and (3) simultaneous diffusion and chemical reaction in the catalyst particle with Michaelis–Menton kinetics and a reliable diffusion model (Zhao and DeLancey in Biotechnol Bioeng 64:434–441, 1999, 2000). The solution to the mathematical model was obtained with Mathematica utilizing the Runge Kutta 4–5 method. The dimensionless length resulting from the continuous solution was compared with the optimal length restricted to a uniform or constant cell loading across the entire bed. The maximum difference in the dimensionless length between the continuous and uniform solutions was determined to be 6.5%. The model was applied to published conversion data for the continuous production of ethanol that included cell loading (Taylor et al. in Biotechnol Prog 15:740–751, 2002). The data indicated a minimum production cost at a catalyst loading within 10% of the optimum predicted by the mathematical model. The production rate versus cell loading in most cases displayed a sufficiently broad optimum that the same (non-optimal) rate could be obtained at a significantly smaller loading such as a rate at 80% loading being equal to the rate at 20% loading. These results are particularly important because of the renewed interest in ethanol production (Novozymes and BBI International, Fuel ethanol: a technological evolution, 2004).

Keywords Biocatalyst · Cell loading · Diffusion · Optimization · Uniform · Continuous · Mathematical model

List of symbols

$C_{A\infty}$	feed concentration of substrate in bulk phase
C	dimensionless bulk phase concentration of substrate as fraction of feed concentration
C_{p}	dimensionless pellet phase concentration of substrate as fraction of feed concentration
D_{ab}	diffusivity of substrate in bulk fluid phase
D_{aA}	axial dispersion coefficient of substrate
D_{eA}	effective diffusivity of substrate through the cell–gel system
D_{e0}	effective diffusivity of substrate in the gel
D_{c}	effective diffusivity of substrate through the cell
j_{D}	$\frac{k_{\mathrm{c}}}{v} Sc^{2/3}$, dimensionless mass transfer factor
K_{p}	distribution coefficient between the mixture in the pores and the cell
$\hat{K}_{\mathrm{p}}$	$\frac{K_{\mathrm{p}} D_{\mathrm{c}}}{D_{\mathrm{e0}}}$, dimensionless diffusion–partition parameter
K_{m}	parameter in Michaelis–Menton kinetics expression
$\hat{K}_{\mathrm{m}}$	$\frac{K_{\mathrm{m}}}{C_{A\infty}}$, dimensionless parameter in Michaelis–Menton kinetics expression
k_{c}	mass transfer coefficient in terms of concentration
$\hat{L}$	dimensionless length of reactor relative to half thickness of pellet

V. Tortoriello · G. B. DeLancey (✉)
Chemical Engineering Program, Stevens Institute of Technology, Hoboken, NJ 07030, USA
e-mail: gdelance@stevens.edu

L_p half thickness of slab
Pe $\frac{vL_p}{D_{aA}}$, Peclet number
r_{max} maximum rate parameter in Michaelis–Menton kinetics expression
Re $\frac{\rho L_p v}{\mu}$, Reynolds number
Sc $\frac{\mu}{\rho D_{ab}}$, Schmidt number
v superficial velocity of bulk fluid phase
z dimensionless axial distance from bed entrance relative to half thickness of pellet

Greek symbols

ε_b void fraction of packed bed
η fractional distance from center of semi-infinite slab
μ viscosity of bulk fluid phase
ρ density of bulk fluid phase
ϕ_c volume fraction of cells in catalyst particle
Φ $L_p^2 \frac{r_{max}}{c_{A\infty} D_{e0}}$, modified Thiele modulus

Introduction

The immobilization of microorganisms in a defined volume with retention of their catalytic activities for repeated and continued use is a common practice in bioreactor operation [7, 13]. The most common and effective methods for cell immobilization include gel entrapment, membrane enclosure and cross linking. Cell immobilization technology provides high cellular concentration and productivity compared with the conventional batch fermentation method where free cells are suspended in a fluid. Immobilization makes it possible to maintain the cells in a stable and viable state, thus providing the means for continuous fermentation [5, 7, 12].

Cell immobilization leads to high reaction rates by virtue of high cell loadings, i.e., the number of embedded cells per unit volume, of the support material. The possibility of using higher cell concentrations in immobilized cell reactors than in fermentors with free cells makes it possible to work under washout conditions where biomass removal rate exceeds the biomass formation rate and increases volumetric productivity. However, the benefits of a high concentration of cells in the immobilization system is partly offset by the diffusional resistance of the dense matrix composed of the cells and the polymeric network of the supporting gel. Diffusional rates will decrease as cell loading increases, thus decreasing the apparent steady state reaction velocity. This inherent competition between the reaction and diffusion rates raises the question as to the most advantageous amount of cells to be incorporated into the support matrix. The subject of this communication is the determination of the optimal cell loading for a fixed bed bioreactor operating at steady state and the practical implementation of this loading.

Modeling

The diffusion component of the reaction–diffusion process within the biocatalyst matrix can be realistically represented by a recent formulation of the effective diffusivity based on the random pore model [11, 12, 15]:

$$\frac{D_{eA}}{D_{e0}} = (1-\phi_c)^2 + \phi_c^2 \frac{K_p D_c}{D_{e0}} + 4\phi_c(1-\phi_c)\frac{\frac{K_p D_c}{D_{e0}}}{1+\frac{K_p D_c}{D_{e0}}}. \quad (1)$$

The model provides for a quadratic dependence of the effective diffusivity on the cell loading with a single physical parameter, $\hat{K}_p = \frac{K_p D_c}{D_{e0}}$. The overall effective diffusivity of reactant in the immobilized cell biocatalyst, D_{eA}, is based on the total cross sectional area. D_{e0} is the effective diffusivity in the support matrix alone, D_c effective diffusivity in the cells, φ_c cell loading or the volume fraction of the cells in the catalyst particle. The partition coefficient, K_p, is defined as the ratio of the average intracellular concentration to the extra cellular concentration between the support gel and the embedded cell [13]. The model is able to correlate a wide range of diffusion data [15].

This diffusivity expression in Eq. (1), coupled with reversible first order and Michaelis–Menten kinetics [15] in a reaction–diffusion model predicts that the optimal cell loading depends on the surface conditions of the cell matrix and exists well within the range of practical interest. The optimal cell loading is presented as a function of the Thiele modulus and provides a general rule of thumb namely that the cell loading should be greater than 1/3 regardless of the kinetic and diffusional resistances [15].

Extension of these results to a fixed bed bio-reactor where the surface conditions of the cell matrix vary continuously along the reaction path is presented here. The investigation was carried out with a transport model that reflects the major mass transfer and reaction regimes in the fixed bed; the bulk flow regime surrounding the catalyst pellet and the diffusion–reaction regime inside the pellet. Mass conservation is expressed in terms of the macro-geometry in the bulk flow regime and in terms of a micro geometry for intrapellet mass transfer with reaction. In this manner, the pellet surface is assumed to be in contact with a uniform fluid phase at one position in the macro-geometry.

The two regimes are uncoupled by determining, a priori, the bulk phase composition required to provide a mass transfer rate equal to the reaction rate in the biocatalyst at a prefixed value of the surface concentration.

Dimensionless equations and solution: overview

The flow of material through the bulk phase over the surface of a catalyst particle involves dispersion, convection, and mass transfer to the surface of the catalyst particle. These are represented respectively with dimensionless variables in Eq. (2):

$$\frac{1}{Pe}\frac{d^2C}{dz^2} - \frac{dC}{dz} - j_D Sc^{-2/3}(1-\varepsilon_b)(C - C_p(1)) = 0. \quad (2)$$

The mass transfer correlations used in this study, $j_D(Re)$, are given in Table 1. The boundary conditions for Eq. (2) are

$$C - \frac{1}{Pe}\frac{dC}{dz} = 1 \quad \text{at } z = 0 \quad (3)$$

$$C = 0.05 \quad \text{at} = \hat{L}. \quad (4)$$

Equation (3) is Danckwerts' condition at the bed entrance and allows for a contribution from the dispersion mechanism at that position which is not present in the region before the bed. The second condition, Eq. (4) can be interpreted as a definition of the reactor length. This set of equations yields a solution in the form of:

$$C = C(z, \varepsilon_b, Pe, Re, Sc, C_p(1), \hat{L}). \quad (5)$$

The substrate concentration distribution within a catalyst particle is the solution to the dimensionless differential mass balance with Michaelis–Menton kinetics:

$$\frac{d^2C_p}{d\eta^2} - \Phi\frac{\phi_c}{D(\phi_c, \hat{K}_p)}\frac{C_p}{(\hat{K}_m + C_p)} = 0. \quad (6)$$

The left hand side of Eq. (1) is denoted by $D(\phi_c, K_p)$. The parameter Φ is a modified Thiele parameter and a measure of the reaction rate relative to the diffusion rate in the catalyst particle. Equation (6) is written for a semi-infinite flat slab. It is well known that catalyst effectiveness can be calculated for arbitrary shapes with this model provided that the external surface to volume ratio of the actual geometry is taken as the thickness of the slab [4].

Symmetry at the center of the slab requires that:

$$\frac{dC_p}{d\eta} = 0 \quad \text{at } \eta = 0. \quad (7)$$

Continuity of the mass transfer rate across the exterior surface of the slab is expressed by

$$j_D Sc^{-2/3}(C - Cp(1)) = \frac{1}{Pe}\frac{dC_p}{d\eta} \quad \text{at } \eta = 1 \quad (8)$$

Equations (7) and (8) require that:

$$C_p(1) = F(\phi_c(z), C, Pe, Re, Sc, \hat{K}_m, \hat{K}_p, \Phi). \quad (9)$$

The catalyst loading is uniform in the pellet but may vary with the axial location in the bed. The two results represented by Eqs. (5) and (9) may be combined to give the reactor length required for a conversion of 95% as a function of the catalyst loading and the dimensionless quantities which characterize the bioreactor:

$$\hat{L} = \hat{L}(\phi_c(z), \varepsilon_b, Pe, Re, Sc, \hat{K}_m, \hat{K}_p, \Phi). \quad (10)$$

The optimization problem can then be stated as follows: Find ϕ_c^{opt} such that:

$$\underset{\phi_c(z)}{Min}[\hat{L}(\phi_c(z), \varepsilon_b, Pe, Re, Sc, \hat{K}_m, \hat{K}_p, \Phi)]. \quad (11)$$

The constraint that $C = 0.05$ is understood in the expression for the reactor length as discussed above. The solution can therefore be represented as

$$\hat{L}_{opt} = \hat{L}_{opt}(\varepsilon_b, Pe, Re, Sc, \hat{K}_m, \hat{K}_p, \Phi). \quad (12)$$

Equations (5) and (9) for C and $C_p(1)$ may be combined at the optimal conditions to produce the final form of the solution for the dimensionless bulk phase concentration, C

$$C_{opt} = C_{opt}(z, \varepsilon_b, \hat{L}, Pe, Re, Sc, \hat{K}_m, \hat{K}_p, \Phi). \quad (13)$$

Table 1 Correlation for external mass transfer coefficients [3]

Correlation	Re range
$j_D = 2.19\ (Re)^{-2/3}$	$0.6 < Re < 50$
$j_D = 2.19\ (Re)^{-2/3} + 0.78\ (Re)^{-0.381}$	$Re > 50$

Calculation procedure

It is apparent that the optimal reactor performance, is determined by the values of seven dimensionless groups: $\varepsilon_b, Pe, Re, Sc, \hat{K}_m, \hat{K}_p, \Phi$. After setting these values, the calculations were carried out as follows:

Equations (2) and (6) are coupled by the mass transfer boundary condition at the surface of the catalyst particle. These equations can be uncoupled by determining the functional relationship between the bulk phase concentration and the interfacial composition at the surface of the catalyst particle, which guarantees satisfaction of the mass transfer boundary condition at the surface of the catalyst particle. This functional relationship when substituted into

Eq. (2), the bulk equation, replaces the need for the simultaneous solution of Eq. (6). The functional relationship was determined in tabular form in four steps:

1. Replace the mass transfer condition at the surface of the catalyst particle with a specified concentration, $C_p(1)$, less than or equal to the feed composition.
2. Solve Eq. (6) and use the results to compute the reaction rate in the catalyst particle.
3. Set the reaction rate equal to the mass transfer rate which was replaced in step 1.
4. Solve the equality in step 3 for the bulk phase composition, C, that must accompany the specified concentration at the surface of the catalyst particle.

In this manner, $C_p(1)$ was constructed as a function of C. Substitution of this function of C into Eq. (2) provides a single differential equation for the bulk phase composition. Equation (2) was solved in this closed form with the specified boundary conditions using the Runge Kutta 4–5 method in Mathematica.

In order to test the validity of the numerical technique, a comparison was made between the known analytical solution and the mathematical model presented in this study with the following conditions:

(a) no axial dispersion (high flow rate, i.e., ranges of high Reynolds number),
(b) no external mass transfer resistance,
(c) an irreversible first order reaction,
(d) internal diffusion resistance and
(e) isothermal reaction.

The two solutions agreed to within a root mean square error of 2.75×10^{-6}. Although a partial comparison of some of the very basic features of convection and internal diffusion with heterogeneous reaction, the results were positive.

Results

Two optimization scenarios, the continuous solution and the uniform solution, were investigated over the range of values used for the dimensionless groups given in Table 2. The most important parameters are those that reflect bulk flow of the material through the reactor and reaction rate in the catalyst particles. The results are therefore represented as functions of Φ (a measure of the reaction rate relative to the diffusion rate in the catalyst) and Re (Reynolds number, a parameter that represents bulk flow). Realistic conversions are guaranteed since the value of $\hat{L}$ was determined in each case to give 95% conversion of the substrate. The different cases are therefore determined by the values of $\varepsilon_b, Pe, Sc, \hat{K}_m$, and $\hat{K}_p$.

Table 2 Range of values used for dimensionless groups

Group	Range	Reference (for range of values)
Geometry		
ε_b	0–1	[4]
$\hat{L}$	100–1,000	
Bulk flow		
Pe	1–2	[1]
Re	10–5,000	
Kinetics		
$\hat{K}_m$	0.1–1,000	[2]
Φ	0.01–1,000	
Diffusion		
$\hat{K}_p$	0–2	[4, 6]
Sc	0.1–0.8	

The continuous solution was obtained by maximizing the reaction rate over each pellet length along the reactor by choosing the catalyst loading that maximized the local reaction rate. A trial and error procedure was followed in each case whereby the optimal cell loading was selected from a range of trial values in order to maximize reaction rate. The accuracy was limited to two significant figures which will not compromise practical implementation of the results. Figure 1 represents solutions for different values of the Reynolds number for the specified values of the parameters. These results are typical and show that the optimal cell loading decreases along the length of the reactor.

The most expedient policy is the single uniform stage. This is referred to as the uniform solution wherein a single optimum loading was determined for the entire bed. A summary of comparisons of the uniform with the contin-

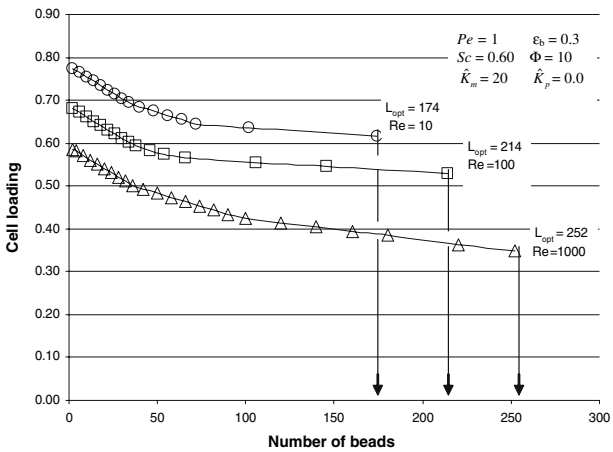

Fig. 1 Optimal cell loading as a function of the dimensionless reactor length

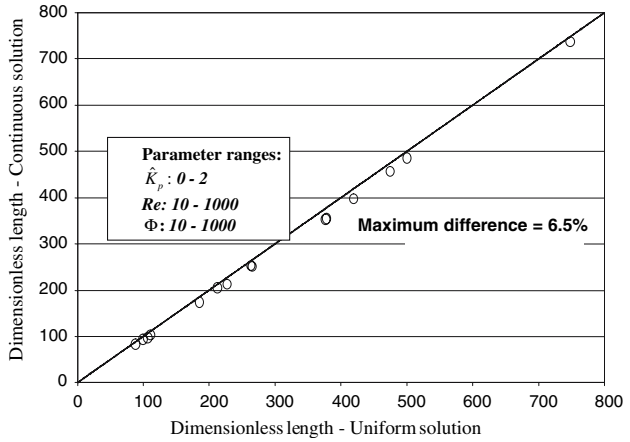

Fig. 2 Comparison of the continuous and uniform solutions

uous solution is shown in Fig. 2. The optimal length from the continuous solution is at most 6.5% less than the uniform solution. It would not therefore be advantageous in the present cases to search for an improvement over the uniform solution. Sectioning the reactor and varying the cell loading stepwise could be investigated in other applications.

Three dimensional graphs illustrating the optimal behavior of the uniform cell loading are displayed in Figs. 3 and 4 for two sets of the fixed parameters. These results illustrate the optimal cell loading for various practical values of ranges of Thiele modulus and Reynolds number at fixed values of the porosity, Peclet number, rate constant and Schmidt number. Each figure is representative of a fixed value of $\hat{K}_p$, which lies within the limits of its practical ranges and for a conversion of 95%. Additionally, the value of the optimal cell loading predicted [15] for L-trytophan synthesis using immobilized E. coli is shown in Fig. 3 [15].

Discussion

The results in Fig. 3 show that the optimum cell loading decreases with Thiele modulus except for a constant region at low Reynolds numbers. The onset of that decrease in optimal cell loading is a function of the Thiele modulus and starts in a region beginning at a Reynolds number of 10 and ending at a Reynolds number of 50. The Thiele modulus is inversely proportional to the square root of the effective diffusivity. This effect is indicated by the higher values of optimal cell loading in the area of low Thiele modulus. Additionally, a small Thiele modulus means diffusion resistance has less of an effect on the reaction and therefore, the optimal cell loading becomes higher. The optimal cell loading corresponds to the diffusional (resistance) limitations. Consequently, as the Thiele modulus is

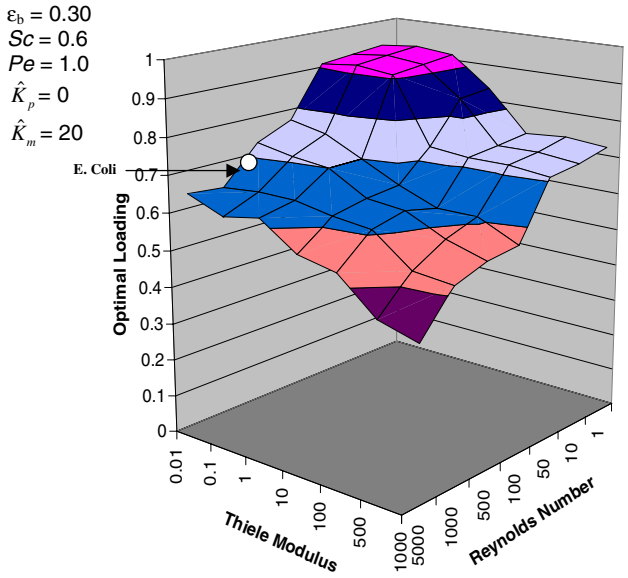

Fig. 3 Optimal cell loading versus modified Thiele modulus and Reynolds number with experimental data shown for *E. coli* data [7]

increased the effects of diffusion resistance lower the optimal cell loading in this region. This pattern is consistent as the value of $\hat{K}_p$ increases. The Thiele modulus used in this study is a modified Thiele modulus to make it independent of cell loading and to interpret it as a direct measure of reaction rate relative to the diffusion rate in the catalyst.

The results further show, the optimal cell loading decreasing as the Reynolds number increases except for a

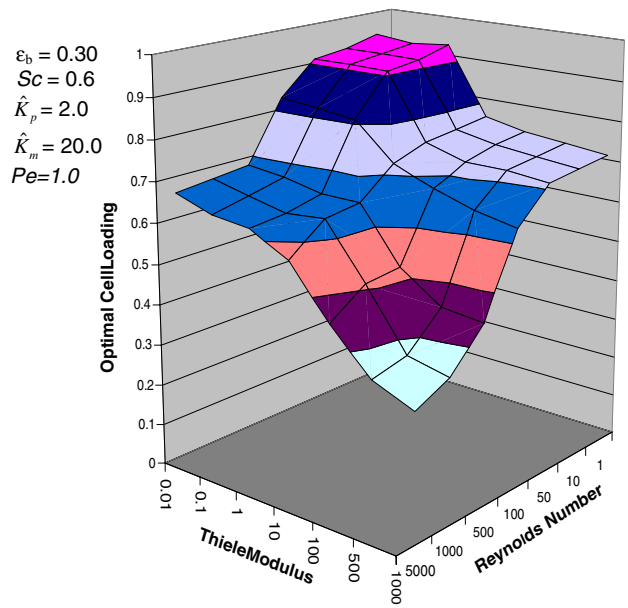

Fig. 4 Optimal cell loading versus modified Thiele modulus and Reynolds number

constant region in the low ranges of Reynolds number. As the Thiele parameter decreases the diffusion rate is increasing which means that a higher mass transfer coefficient in the external region is required to match the internal diffusion rate. This requires a higher Reynolds number as found in this study.

In the high ranges of Thiele modulus and Reynolds number there was a slight decrease in the optimal cell loading as $\hat{K}_p$ was increased, but in the low ranges of both values no discernable change in the optimum cell loading was detected as the value of $\hat{K}_p$ was increased. This indicates that the ratio of the intracellular concentration to extra cellular concentration has little effect on the optimal cell loading of this system.

Additionally, one example of a dimensionless reaction rate of 0.143 was calculated for loadings of both 0.19 and 0.78 during the optimization study when determining the maximum reaction rate in the continuous solution. This result is indicative of a broad peak in reaction rate versus cell loading.

Comparison with production cost

Operating data for the conversion of sugar to ethanol in a fixed bed containing immobilized yeast that include the cell loading are available from a recent study [9]. Actual data from the SERI Corporation were utilized to plot the production cost versus cell loading [9, 10]. The results are shown in Figs. 5, 6, and 7.

In each case a minimum in the production cost is displayed. For conversions of 72, 80 and 85%, respectively,

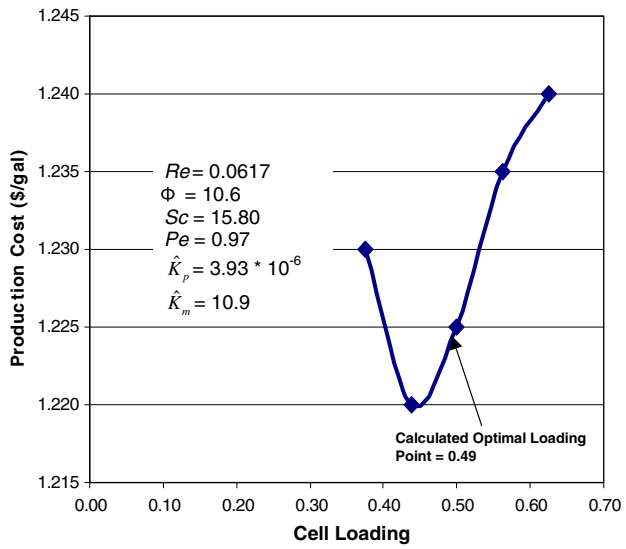

Fig. 5 Production cost analysis from an industrial survey indicating the optimal cell loading point for 72% conversion [10]

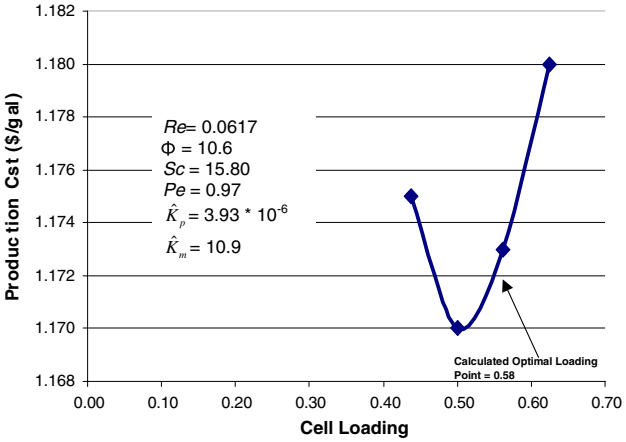

Fig. 6 Production cost analysis from an industrial survey indicating the optimal cell loading point for 80% conversion [10]

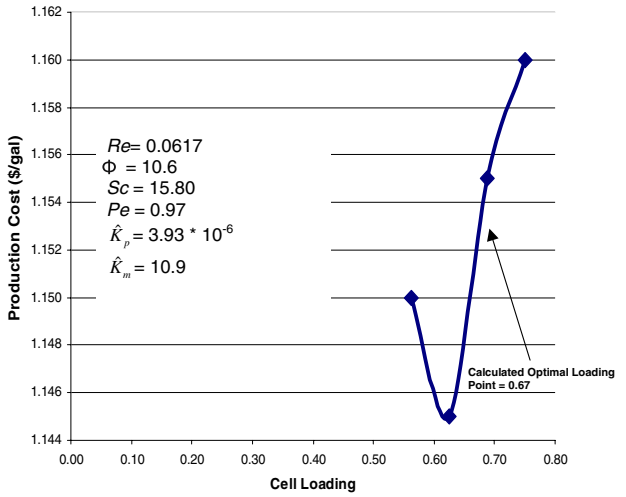

Fig. 7 Production cost analysis from an industrial survey indicating the optimal cell loading point for 85% conversion [10]

the cost of ethanol production varies from a high of $1.22/gal at 72% conversion, to $1.17 for 80% conversion and finally $1.15 for 85%. The associated operating conditions which are also shown in the figures were used in the present model to compute optimal cell loadings. The calculated cell loadings are seen to closely approximate the location of the minima in the production cost.

Conclusion

This study confirmed the existence of an optimal cell loading of microbial catalyst an inert support in a fixed bed of resting cells. The optimal cell loading may be reflected by a minimum in the bed length for a fixed conversion or by a maximum in the conversion for a fixed length. The

optimum loading generally varies with axial position along the length of the reactor. However, it was found that over the range of practical values investigated there is no significant difference from an optimal loading policy independent of axial position. It was found that the major parameters that affect the results and the optimum loading policy are the Reynolds number and the Thiele modulus.

An economic analysis on the effects of cell loading on actual production costs from an industrial survey displayed a good correlation between the minimums found in that study with the optimal loading established in this study. This emphasizes the vital role of factors such as amount of catalyst, size of reactor, residence time and operating conditions in optimization of production costs.

References

1. Aris R, Amundson N (1957) Some remarks on longitudinal mixing or diffusion in fixed beds. AICHE J 3(2):280–291
2. Bailey JE, Ollis DF (1986) Biochemical engineering fundementals, 2nd edn. McGraw-Hill Inc., New York
3. Bird RB, Stewart WE, Lightfoot EN (2002) Transport phenomena. Wiley, New York
4. Froment GF, Bischoff KB (1990) Chemical reactor analysis and design, 2nd edn. Wiley, New York
5. Furusaki S, Seki M, Wang H (1995) Evaluation of co-immobilized *Lactobacillus delbruecki* with porous particles for lactic acid production. J Chem Eng Jpn 29:1 37–43
6. Indlekofer M, Brotz F, Bauer A, Reuss M (1996) Stereo selective bioconversions in continuously operated fixed bed reactors: modeling and process optimization. Biotechnol Bioeng 52:459–471
7. Libicki SB, Salmon PM, Robertson CR (1988) The effective diffusivity permeability of a non-reacting solute in microbial cell aggregates. Biotechnol Bioeng 32:68–85
8. Novozymes and BBI International (2004) Fuel ethanol: a technological evolution
9. Taylor F (2000) Control of the packed fouling in the continuous fermentation and stripping of ethanol. Biotechnol Prog 16:541–547
10. Taylor F, Mcaloon A, Craig J (2002) Operating cost for fuel ethanol production by continuous ethanol fermentation and stripping and comparison with existing technology. Biotechnol Prog 15:740–751
11. Wakao N, Smith JM (1962) Diffusion in catalyst pellets. Chem Eng Sci 17:825–834
12. Wakao N, Smith JM (1964) Diffusion and reaction in porous catalysts. I&EC Fundam 3:123–127
13. Westrin BA, Axelsson A (1991) Diffusion in gels containing immobilized cells: a critical review. Biotechnol Bioeng 38:439–446
14. Zhao Y, DeLancey GB (1999) Transmembrane distribution of substrate and product during the bioreduction of acetophenone with resting cells of *Saccharomyces cerevisiae*. Biotechnol Bioeng 64:434–441
15. Zhao Y, DeLancey GB (2000) A diffusion model and optimal cell loading for immobilized cell biocatalyst. Biotechnol Bioeng 64:434–441